Inorg. Chem. **2006**, *45*, 6263–6268

Synthesis, Structure, and Anticancer Activity of Gallium(III) Complexes with Asymmetric Tridentate Ligands: Growth Inhibition and Apoptosis Induction of Cisplatin-Resistant Neuroblastoma Cells

Rajendra Shakya,[†] Fangyu Peng,*[,‡] Jianguo Liu,[‡] Mary Jane Heeg,[†] and Claudio N. Verani*[,†]

Department of Chemistry, Wayne State University, 5101 Cass Avenue, Detroit, Michigan 48202, and Carman & Ann Adams Department of Pediatrics, Department of Radiology, and Barbara Ann Karmanos Cancer Institute, Wayne State University School of Medicine, 3901 Beaubien Boulevard, Detroit, Michigan 48201

Received January 18, 2006

Five gallium(III) complexes described as $[Ga^{III}(L^X)_2]ClO_4$, where $(L^X)^-$ is the deprotonated form of a series of asymmetric ligands containing pyridine and 4,6-substituted phenol moieties, were synthesized and characterized by spectroscopic and spectrometric methods. Phenol substituents encompass the electron-withdrawing and electron-donating methoxy (**1**), nitro (**2**), chloro (**3**), bromo (**4**), and iodo (**5**) groups. Complexes **1** and **3** have had their molecular structure solved by X-ray crystallography and show distinct coordination modes. Complexes **1**–**5** were tested for growth-inhibition activity on cisplatin-resistant human neuroblastoma cells; those containing halogen substituents on the phenolate rings, i.e., **3**–**5**, showed activity superior to that observed for cisplatin and induced apoptosis of neuroblastoma cells. Nitro-containing **2** suppressed proliferation of the neuroblastoma cells but induced apoptosis less effectively.

Introduction

Neuroblastoma is a malignant tumor of the peripheral sympathetic nervous system found in children. It accounts for one in every eight to ten cases of childhood cancer.[1] Currently, neuroblastoma is treated with a combination of surgery, radiation therapy, and chemotherapy.[2] Chemotherapeutic drugs for the treatment of neuroblastoma include platinum-containing agents, such as cisplatin and carboplatin. Despite an initial good response, resistance develops rapidly and results in relapse and treatment failure.[3] Although efforts have been made,[4] new drugs effective in treating cisplatin-resistant neuroblastoma are urgently needed to improve the chances of survival in children suffering from this disease. One of the major difficulties encountered in anticancer drug development is nonspecific toxic effects on normal cells or tissues. Promising approaches for overcoming such undesirable side effects encompass the development of targeted drug delivery to specific tumor tissues and the use of markers for in vivo tracking of tumor inhibition and apoptosis.[5] Nuclear imaging techniques especially useful for tracking targeted drug delivery in vivo are single photon emission computed tomography (SPECT) and positron emission tomography (PET) because of their high sensitivity, capability for quantitative analysis, and noninvasive nature.[6]

Our groups are interested in the development of complexes formed between organic ligands and γ-ray or positron-emitting gallium radionuclides (^{67}Ga for SPECT or ^{68}Ga for PET) that could allow for imaging and therapy of these diseases. Driven by this premise, as well as by the established therapeutic activity of gallium(III) complexes,[7−10] we present

* To whom correspondence should be addressed. E-mail: cnverani@chem.wayne.edu (C.N.V.). Fax: (313) 577-8822 (C.N.V.).
[†] Department of Chemistry, Wayne State University.
[‡] Wayne State University School of Medicine.

(1) Olshan, A. F.; Bunin, G. R. *Neuroblastoma*; Brodeur, G. M., Sawada, T., Tsuchida, Y., Voute, P. A., Eds.; Elsevier: New York, 2000; p 33.
(2) Niethammer D.; Handgretinger, R. *Eur. J. Cancer* **1995**, *31A*, 568.
(3) Andrews, P. A. *Anticancer Drug Resistance*; Goldstein, L. J., Ozols, R. F. Eds.; Kluwer Academic: Boston, 1994; p 217.
(4) Bernstein, M. L.; Reaman, G. H.; Hirschfeld, S. *Hematol. Oncol. Clin. North Am.* **2001**, *15*, 631.
(5) Jain, R. K. *Clin. Cancer Res.* **1999**, *5*, 1605.
(6) Wang, J.; Maurer, L. *Curr. Top. Med. Chem.* **2005**, *5*, 1053.
(7) Dobrov, A.; Arion, V. B.; Kandler, N.; Ginzinger, W.; Jakupec, M. A.; Rufinska, A.; von Keyserlingk, N. G.; Galanski, M.; Kowol, C.; Keppler, B. K *Inorg. Chem.* **2006**, *45*, 1945.
(8) Bernstein, L. R. *Metallotherapeutic Drugs and Metal-Based Diagnostic Agents*; Gielen, M., Tiekink, E. R. T., Eds.; Wiley: Weinheim, Germany, 2005, 259.
(9) Bernstein, L. R. *Pharmacol. Rev.* **1998**, *50*, 665.

10.1021/ic060106g CCC: $33.50
Published on Web 07/12/2006

Scheme 1

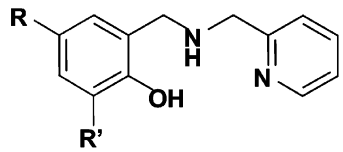

$[Ga^{III}(L^{MeO})_2]ClO_4$	**(1)**	R = *H*, R' = *methoxy*
$[Ga^{III}(L^{NO2})_2]ClO_4$	**(2)**	R = *nitro* and R' = *H*
$[Ga^{III}(L^{Cl2})_2]ClO_4 \cdot MeOH$	**(3)**	R and R' = *chloro*
$[Ga^{III}(L^{Br2})_2]ClO_4$	**(4)**	R and R' = *bromo*
$[Ga^{III}(L^{I2})_2]ClO_4$	**(5)**	R and R' = *iodo*

here the first results toward potent antineuroblastoma drugs based on complexes with asymmetric tridentate NN′O ligands. Phenolate groups are used in the ligand design to allow for the presence of a range of ring substituents and to limit the need for counterions in charge balance. Additionally, these organic species can be synthetically modified to enhance their water solubility by attaching groups to the amine nitrogen.[11] We have synthesized and characterized five complexes, depicted in Scheme 1, with the aim of understanding the role played by the metal ion, the presence of several electron-donating and -withdrawing substituents, and the coordination modes of the ligands in the effective treatment against cisplatin-resistant neuroblastoma cells. Complexes **1**−**5** were characterized by elemental, spectroscopic, and spectrometric methods. Molecular structures were solved by X-ray crystallography for **1** and **3**. Biological assays included tumor-cell growth inhibition, cytopathological effects, and apoptosis induction.

Experimental Section

General. Reagents and solvents were used as received from commercial sources. Methanol was distilled over CaH_2 and dichloromethane was purified via alumina columns in an IT solvent purification system. Infrared spectra were measured from 4000 to 400 cm^{-1} as KBr pellets on a Tensor 27 FT-IR spectrophotometer. ^1H NMR spectra of the ligands were measured using a Varian 400 MHz instrument, and ESI (positive) mass spectra were measured in a triple quadrupole Micromass QuattroLC spectrometer with an electrospray/APCI source. Simulations of peak positions and isotopic distributions were performed with software provided by the manufacturer. Water solubility (S_w) is expressed both in grams and moles per liter and indicates the difference between the initial and undissolved mass of the complexes added to water at 22 °C. Elemental analyses were performed by Midwest Microlab, Indianapolis, IN. The synthesis of the ligands was achieved by Schiff condensation of aminomethyl pyridine with the appropriate aldehyde followed by reduction with $NaBH_4$, as published elsewhere.[12,13] BE(2)-C cells were purchased from American Type Culture Collection (ATCC, Manassas, VA), which were derived from a subclone of SK-N-BE(2) human neuroblastoma cell line and were highly resistant to cisplatin and other platinum chemotherapeutic drugs. The cells were cultured in a 1:1 mixture of EMEM:F12 medium (Biosource International, Camarillo, CA) supplemented with fetal bovine serum (10%, v/v), penicillin (100 units/mL), streptomycin (100 μg/mL), and glutamine (100 μg/mL) at 37 °C in an atmosphere of 5% CO_2. Human fibroblasts established from benign prostate soft tissue post-radical prostectomy for prostate cancer were obtained from the Cell Bank at Karmanos Cancer Institute (Detroit, MI) and cultured in RPMI 1640 medium supplemented with fetal bovine serum, antibiotics, and glutamine, as described above.

X-ray Structural Determinations. Diffraction data were measured on a Bruker X8 APEX-II kappa geometry diffractometer with Mo radiation and a graphite monochromator. Frames were collected as a series of sweeps with the detector at 40 mm and 0.2−0.3 degrees between each frame. Frames were recorded for 2−5 s. APEX-II[14] and SHELX-97[15] software were used in the collection and refinement of the models. Complex **1** crystallized as colorless rods. The sample used for data collection was approximately 0.35 × 0.203 × 0.18 mm^3. A total of 1481 frames were collected at 100 K yielding 27 517 reflections, of which 8760 were independent. Hydrogen positions were placed in observed or calculated positions. No solvent was present in the crystal. The asymmetric unit contains two cationic half-complexes occupying inversion centers and one perchlorate anion. Complex **3** appeared as pale yellow rods, and a sample approximately 0.48 × 0.18 × 0.16 mm^3 was used for room-temperature data collection. A total of 4653 frames were collected, yielding 60 760 reflections, of which 9546 were independent. Hydrogen positions were placed in observed or calculated positions. The asymmetric unit consists of one complex cation, one perchlorate anion and one methanol solvate. Typical large thermal parameters are evident in the perchlorate oxygen atoms.

Synthesis of the Complexes. A general synthetic route was used for **1**−**5** in which a solid sample of anhydrous $GaCl_3$ (0.17 g, 1.0 mmol) was dissolved in 2.0 mL of MeOH inside a glovebox and then added to a 30 mL MeOH solution containing the appropriate ligand (2.0 mmol) and Et_3N (0.28 mL; 2.0 mmol). The resulting yellowish solution was stirred at room temperature for 1 h, and an excess of sodium perchlorate was then added to exchange chloride by perchlorate counterions. After 24 h, off-white microcrystalline precipitates were frit-filtered, washed with cold water and ethyl ether, and then recrystallized in MeOH by slow evaporation.

$[Ga^{III}(L^{MeO})_2]ClO_4$ (1). Yield after recrystallization: 76%. Elemental anal. Calcd for $C_{28}H_{30}N_4Cl_1O_8Ga_1$: C, 51.29; H, 4.61; N, 8.44. Found: C, 51.50; H, 4.69; N, 8.34. IR data (KBr, cm^{-1}): 1085 (Cl−O from ClO_4^-), 3292 (N−H stretches). MS data (ESI(+) in MeOH): *m*/*z* 555 for $[Ga^{III}(L^{MeO})_2]^+$. S_w: 0.805 g/L, 1.23 × 10^{-3} mol/L.

$[Ga^{III}(L^{NO2})_2]ClO_4$ (2). Yield after recrystallization: 71%. Elemental anal. Calcd for $C_{26}H_{24}N_6Cl_1O_{10}Ga_1$: C, 45.54; H, 3.53; N, 12.16. Found: C, 46.92; H, 3.54; N, 12.16. IR data (KBr, cm^{-1}): 1092 (Cl−O from ClO_4^-), 1302(s) (N═O stretch from nitro groups). MS data (ESI(+) in MeOH): *m*/*z* 585 for $[Ga^{III}(L^{NO2})_2]^+$. S_w: 0.115 g/L, 1.68 × 10^{-4} mol/L.

$[Ga^{III}(L^{Cl2})_2]ClO_4$(3). Yield after recrystallization: 79%. Elemental anal. Calcd for $C_{27}H_{26}N_4Cl_5O_7Ga_1$: C, 42.36; H, 3.42; N, 7.32. Found: C, 42.10; H, 3.49; N, 7.23. IR data (KBr, cm^{-1}): 1109 (Cl−O from ClO_4^-), 3244 (N−H stretches). MS data

(10) Harpstrite, S. E.; Beatty, A. A.; Collins, S. D.; Oksman, A.; Goldberg, D. E.; Sharma, V. *Inorg. Chem.* **2003**, *42*, 2294.
(11) (a) Fulton, D. A.; Elemento, E. M.; Aime, S.; Chaabane, L.; Botta, M.; Parker, D. *Chem. Commun.* **2006**, 1064. (b) Storr, T.; Sugai, Y.; Barta, C. A.; Mikata, Y.; Adam, M. J.; Yano, S.; Orvig, C. *Inorg. Chem.* **2005**, *44*, 2698. (c) Caravan, P.; Ellison, J. J.; McMurry, T. J.; Lauffer, R. B. *Chem. Rev.* **1999**, *99*, 2293.
(12) Imbert, C.; Hratchian, H. P.; Lanznaster, M.; Heeg, M. J.; Hryhorczuk, L. M.; McGarvey, B. R.; Schlegel, H. B.; Verani, C. N. *Inorg. Chem.* **2005**, *44*, 7414 and references therein;
(13) Shakya, R.; Imbert, C.; Hratchian, H. P.; Lanznaster, M.; Heeg, M. J.; McGarvey, B. R.; Allard, M.; Schlegel, H. B.; Verani, C. N. *Dalton Trans.* **2006**, 2517.
(14) *APEX II* collection and processing programs are distributed by Bruker AXS Inc., Madison WI.
(15) Sheldrick, G. *SHELX-97*; University of Göttingen: Göttingen, Germany, 1997.

(ESI(+) in MeOH): *m*/*z* 631 for $[Ga^{III}(L^{Cl2})_2]^+$. S_w: 0.100 g/L, 1.31×10^{-4} mol/L.

$[Ga^{III}(L^{Br2})_2]ClO_4$. (4). Yield after recrystallization: 71%. Elemental anal. Calcd for $C_{26}H_{22}N_4Cl_1O_6\ Br_4Ga_1$: C, 34.27; H, 2.43; N, 6.15. Found: C, 34.19; H, 2.56; N, 6.00. IR data (KBr, cm^{-1}): 1108 (Cl−O from ClO_4^-), 3249 (N−H stretches). MS data (ESI(+) in MeOH): *m*/*z* 807 for $[Ga^{III}(L^{Br2})_2]^+$. S_w: 0.120 g/L, 1.32×10^{-4} mol/L.

$[Ga^{III}(L^{I2})_2]ClO_4$ (5). Yield after recrystallization: 76%. Elemental anal. Calcd for $C_{26}H_{20}N_4Cl_1O_6\ I_4Ga_1$: C, 28.41; H, 2.02; N, 5.10. Found: C, 28.25; H, 1.93; N, 4.96. IR data (KBr, cm^{-1}) 1093 (Cl−O from ClO_4^-), 3292 (N−H stretches). MS data (ESI(+) in MeOH): *m*/*z* 999 for $[Ga^{III}(L^{I2})_2]^+$. S_w: 0.050 g/L, 4.5×10^{-5} mol/L.

Growth Inhibition Assay. The cell-growth inhibitory effect of **1**−**5** was measured by an MTT-based cell proliferation assay.[16] This assay measures the ability of metabolically active cells to convert the yellow tetrazolium salt 3-(4,5-dimethylthiazol-2-yl)-2,5-diphenyltetrazolium bromide (MTT) into a blue cleavage product using an MTT assay kit from Chemicon (Temecula, CA). Cells growing in the logarithmic phase were seeded into a 96-well microplate (1×10^4 cells in 100 μL culture medium/well) 12 h prior to treatment with the gallium(III) complexes. Several concentrations of **1**−**5** were dissolved in 5% DMSO, added to triplicate wells, and incubated at 37 °C for 24 h. Aliquots of 20 μL of MTT solution were then added to each well. After incubation at 37 °C for 4 h, the absorbance of the colored products was recorded at 405 nm with a Spectra Max 250 microplate reader (Molecular Devices, Union City, CA). The growth inhibition was calculated by dividing the average absorbance of the cells treated with a given gallium(III) complex or cisplatin by that of the control (the cells treated with an equal amount of a 95:5 H_2O:DMSO solution, hereafter 5% DMSO); IC 50 values (the drug concentration at which growth of the tumor cells was inhibited to 50% of control) were interpolated from a second-order polynomial fit of growth inhibition. Each experiment was repeated at least three times and each point was determined in triplicate.

Cytopathological Effects Examination. Following drug treatment, the neuroblastoma cells were evaluated for morphological cytopathological effects with an Olympus phase-contrast microscope. The cells treated with equal amounts of 5% DMSO were included as the negative control and cisplatin as the positive control. The cytopathological effects were recorded with an Olympus phase-contrast microscope equipped with a Spot digital camera (Diagnostic Instruments, Sterling Heights, MI). Shrinkage, spherical morphology, and detachment of the treated tumor cells were taken as evidence of cytopathological effects induced by some of the complexes. Additionally, human fibroblasts (Cell Bank, Karmanos Cancer Institute, Detroit, MI) were treated with the gallium(III) complexes to evaluate their effects on nonmalignant human cells.

Apoptosis-Induction Assay. The apoptosis-induction activity of **1**−**5** was evaluated by staining the drug-treated cells with Annexin V-FITC and propidium iodide followed by performing flow cytometry. Annexin V preferentially binds to negatively charged phospholipids present on the cytoplasmic membrane of the tumor cells undergoing apoptosis, whereas propidium iodide stains nuclei of cells undergoing late apoptosis or necrosis. The apoptosis-induction assay was performed with a modification of a previously reported protocol,[17] using a detection kit from R&D Systems (St. Paul, MN). Exponentially growing tumor cells were seeded in a six-well plate (1×10^5 cells/well) and treated with **1**−**5** for 24 h. At the end of the incubation period, the cells were harvested by digestion with 0.25% trypsin and washed with PBS twice. Incubation was followed with an application of a mixture of Annexin V-FITC and propidium iodide for 20 min and cells were analyzed with flow cytometry using an EPICS ALTRA flow cytometer (Beckman Coulter, Fullerton, CA). Apoptosis of the drug-treated cells was further confirmed by nuclear staining with Hoechst 33258 (Sigma, St. Louis, MO), followed by microscopic examination using an Olympus phase-contrast/fluorescence microscope.[18] Strong fluorescence of condensed nuclei following drug treatment indicates cell apoptosis.

Statistical Analysis. To determine whether there is a significant difference in antitumor activity among **1**−**5**, we applied a one-way ANOVA. A *p*-value <0.05 was considered statistically significant.

Table 1. Crystal Data[a]

	1	**3**
formula	$C_{28}H_{30}N_4O_8Cl_1Ga$	$C_{27}H_{26}N_4O_7Cl_5Ga$
fw	655.73	765.49
space group	*P*2(1)/*c*	*P*2(1)/*c*
a (Å)	11.3358(2)	11.1023(2)
b (Å)	17.9930(3)	19.3003(4)
c (Å)	14.1867(2)	15.0171(3)
β (deg)	104.9410(10)	104.5800(10)
V (Å^3)	2795.76(8)	3114.21(11)
Z	4	4
T (K)	100(2)	195(2)
λ (Å)	0.71073	0.71073
D_{calcd} (g cm^{-3})	1.558	1.633
μ (mm^{-1})	1.138	1.364
R(*F*)(%)	3.30	3.94
$R_w(F)$ (%)	8.51	12.02

[a] $R(F) = \sum||F_o| - |F_c|/\sum|F_o|$; $R_w(F) = [\sum w(F_o^2 - F_c^2)^2 / \sum w(F_o^2)^2]^{1/2}$ for $I > 2\sigma(I)$.

Results and Discussion

Syntheses and Characterization. Complexes **1**−**5** were synthesized by treating the respective ligands with anhydrous gallium(III) chloride in dry methanol, followed by performing counterion metathesis with sodium perchlorate. These reactions yielded pseudo-octahedral mononuclear species in which the metal ion was surrounded by two tridentate ligands. The perchlorate counterions were found between 1116 and 1088 cm^{-1}, and ESI mass spectrometry in the positive mode in methanol gave single, well-defined peaks corresponding to $m/z = [Ga^{III}(L)_2]^+$ (100%) for all complexes. These peaks were simulated and showed good agreement in their position and isotopic distributions**.** The other peaks present displayed intensity below 1%. Good elemental analyses were obtained for **1**−**5**.

Molecular Structures. Complexes **1** and **3** have had their structures determined by X-ray crystallography (for crystallographic data, see Table 1. Their ORTEP diagrams are shown in Figure 1 and selected bond lengths and angles are given in Table 2.

$[Ga^{III}(L^{OMe})_2]ClO_4$ (1). Complex **1** crystallizes in monoclinic space group *P*2(1)/*c* with two independent but chemically equivalent cations. The cations are composed of a gallium(III) ion coordinated to two deprotonated $(L^{OMe})^-$ ligands, with each of them containing an $N_{am}N_{py}O_{phen}$ set of

(16) Mosmann, T. *J. Immunol. Methods* **1983**, *65*, 55.
(17) Vermes I.; Haanen, C.; Steffens-Nakken, H.; Reutelingsperger, C. *J. Immunol. Methods* **1995**, *184*, 39.

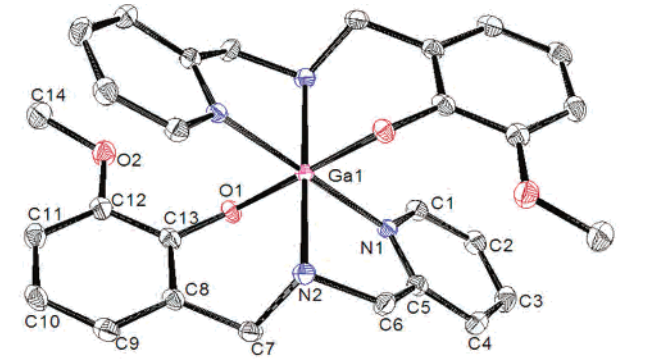

$[Ga^{III}(L^{OMe})_2]ClO_4$ (1)

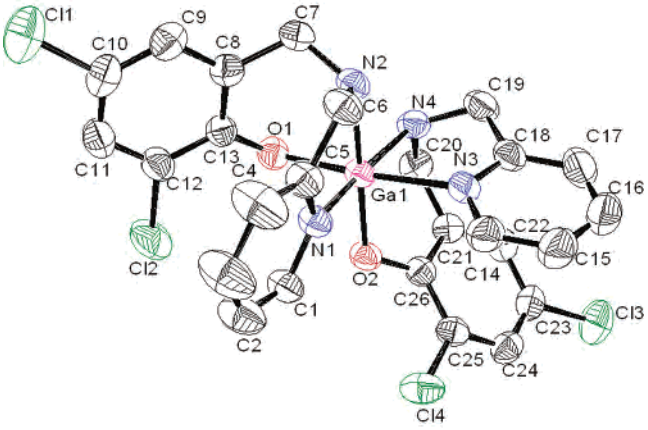

$[Ga^{III}(L^{Cl2})_2]ClO_4$ (3)

Figure 1. ORTEP diagrams at the 50% probability level for **1** and **3**. Counterions, solvents, and hydrogen atoms are excluded for clarity.

Table 2. Selected Bond Distances (Å) and Angles (deg) for **1** and **3**

1		**2**	
Ga(1)−O(1)	1.945(11)	Ga(1)−O(1))	1.932(15
Ga(2)−O(3)	1.926(10)	Ga(1)−O(2)	1.905(13)
Ga(1)−N(2)	2.086(13)	Ga(1)−N(2)	2.129(16)
Ga(1)−N(4)	2.111(13)	Ga(1)−N(4)	2.090(17)
Ga(1)−N(1)	2.093(12)	Ga(1)−N(1)	2.040(16)
Ga(2)−N(3)	2.111(13)	Ga(1)−N(3)	2.150(18)
C(13)−O(1)	1.433(2)	C(13)−O(1)	1.335(3)
C(27)−O(3)	1.346(19)	C(26)−O(2)	1.332(2)
N(2)−C(7)	1.498(19)	N(2)−C(7)	1.492(3)
N(4)−C(21)	1.498(2)	N(4)−C(20)	1.508(3)
C(6)−N(2)	1.487(2)	C(6)−N(2)	1.489(3)
C(20)−N(4)	1.491(2)	C(19)−N(4)	1.483(3)
N(3)−Ga(1)−N(1)	180.00	N(4)−Ga(1)−N(1)	171.25(7)
O(1)−Ga(1)−N(4)	90.70(5)	O(1)−Ga(1)−N(4)	95.90(7)
O(3)−Ga(2)−N(2)	88.86(5)	O(1)−Ga(1)−N(2)	90.53(6)
C(13)−O(1)−Ga(1)	114.34(9)	C(13)−O(1)−Ga(1)	119.93(12)
C(27)−O(3)−Ga(2)	117.69(9)	C(26)−O(2)−Ga(1)	119.92(11)

donors. Both ligands are facially coordinated with the two pyridine rings (Ga−N ≈ 2.09 Å), the two phenolate rings (Ga−O ≈ 1.94 Å), and the two imine groups (Ga−N_{am} ≈ 2.09 Å) arranged trans to one another to yield a pseudo-octahedral geometry. Figure 1a shows the first cation that is described in an adapted Bailar, Miessler, and Tarr notation[19] as [Ga $<N_{am1}N_{am2}>$ $<N_{py1}N_{py2}>$ $<O_{phen1}O_{phen2}>$] and exhibits a D_{2h} local symmetry, if ring orientations are not

(18) Elstein, K. H.; Zucker, R. M. *Exp. Cell Res.* **1994**, *211*, 322.

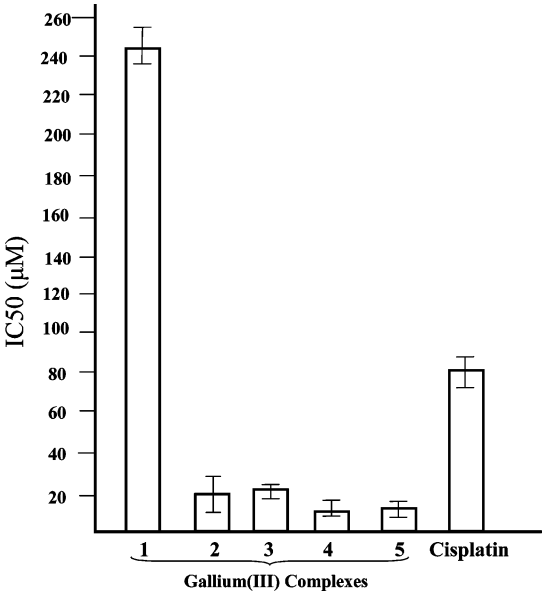

Figure 2. Growth inhibitory effects of the gallium(III) complexes on the BE(2)-C cells. Complex **4** showed the strongest growth inhibition effects followed by **5**, **2**, **3**, and **1**, in a descending order of strength.

considered. Typical values for coordination of such ligands to a gallium(III) ion are observed.[20] A remote perchlorate anion completes the description of **1**.

$[Ga^{III}(L^{Cl2})_2]ClO_4$ (3). Complex **3** also crystallizes in monoclinic *P*21/*c* space group, with the cation showing similar facial coordination of the $(L^{Cl2})^-$ ligands (Figure 1b). A pseudo-octahedral geometry is seen for both **1** and **3**; however, whereas the former exhibits a symmetrical all-trans distribution of the $N_{am}N_{py}O_{phen}$ donor sets, the latter complex is described in an all-cis [Ga $<N_{am1}O_{phen2}>$ $<N_{am2}N_{py1}>$ $<O_{phen1}N_{py2}>$] configuration of C_i local symmetry. Comparable Ga−$O_{phenolate}$ bond lengths are seen for **1** and **3**, whereas shorter Ga−N_{amine} and longer Ga−$N_{pyridine}$ are observed for **3**.

Previously published results for this series of ligands with distinct 3d metals show a good correlation between the preferred coordination modes and the metal centers, independent of the nature of the phenolic substituents if the synthetic conditions are kept unchanged. Therefore, iron(III) complexes display a [Fe $<N_{am1}O_{phen2}>$ $<N_{am2}O_{phen1}>$ $<N_{py1}N_{py2},>$] arrangement,[12] whereas cobalt(III) complexes prefer a [Co $<N_{am1}N_{am2}>$ $<N_{py1}N_{py2}>$ $<O_{phen1}O_{phen2}>$] arrangement[13] similar to that of **1**. Gallium(III) complexes

(19) Adapted from Miessler, G.; Tarr, D. *Inorganic Chemistry*; Pearson−Prentice Hall:Upper Saddle River, NJ, 2004; p 311. The notation $<A_1B_2>$ indicates that A is trans to B, with A and B corresponding to the pyridine (N_{py}), amine (N_{am}), or phenolato (O_{phen}) groups. Subscripts 1 and 2 designate the first and the second ligands, respectively.

(20) (a) Darensbourg, D. J.; Billodeaux, D. R. *C. R. Chim.* **2004**, *07*, 755. (b) Beckmann, U.; Bill, E.; Weyhermüller, T.; Wieghardt, K. *Eur. J. Inorg. Chem.* **2003**, *09*, 1768. (c) Van Aelstyn, M. A.; Keizer, T. S.; Klopotek, D. L.; Liu, S.; Munoz-Hernandez, M.-A.; Wei, P.; Atwood, D. A. *Organometallics* **2000**, *19*, 1796. (d) Brown, M. A.; El-Hadad, A. A.; McGarvey, B. R.; Sung, R. C. W.; Trikha, A. K.; Tuck, D. G. *Inorg. Chim. Acta* **2000**, *300*, 613. (e) Camacho-Camacho, C.; Merino, G.; Martínez-Martínez, F. J.; Nöth, H.; Contreras, R. *Eur. J. Inorg. Chem.* **1999**, *06*, 1021. (f) Wong, E.; Caravan, P.; Liu, S.; Rettig, S. J.; Orvig, C. *Inorg. Chem.* **1996**, *35*, 715. (g) Wong, E.; Liu, S.; Rettig, S.; Orvig, C. *Inorg. Chem.* **1995**, *34*, 3057.

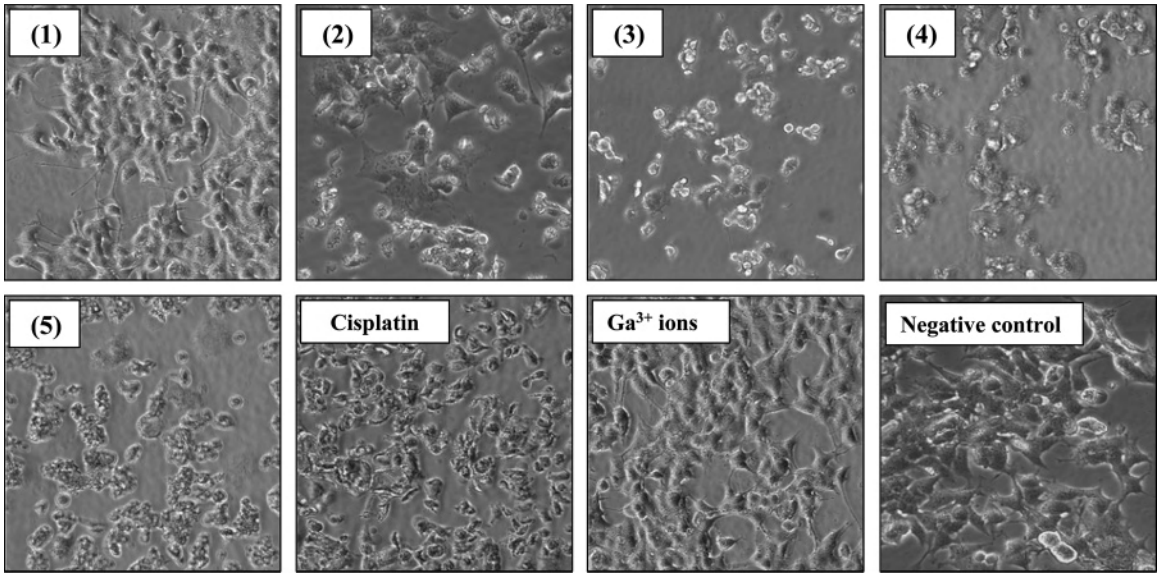

Figure 3. Cytopathological effects (CPE) of gallium(III) complexes on the BE(2)-C neuroblastoma cells. No significant CPE observed on cells treated with **1**, Ga^{3+} ions, or an equal amount of solvent (5% DMSO) in the negative control. Magnification is 200×.

are the only species in which a lack of geometric preference has been observed thus far, which is attributed to the $3d^{10}$ electronic configuration of the ion. Because no empty orbitals are present, the interactions between the ligands and the gallium center are mainly electrostatic in nature and coordination is either randomly achieved or dictated by the solubility of the ligands and the bulkiness of the phenolic substituents.

Growth Inhibition of Neuroblastoma Cells. The complexes tested in this study showed variable growth-inhibition activity on the BE(2)-C neuroblastoma cells (Figure 2). The growth-inhibition activity is plotted by complex as IC50, the concentration at which growth of the cells was inhibited to half that of the control cells treated with an equal amount of solvent (5% DMSO). Complexes **2**−**5** showed strong growth-inhibition effects, with IC50 values of 20.5 ± 4.0, 23.8 ± 4.4, 13.3 + 3.8, and 14.2 ± 4.1 μM, respectively, in comparison to that of cisplatin (IC 50 of 80.3 ± 6.4 μM). Statistical analysis showed a highly significant difference between the IC50 values of complexes **2**−**5** and that of cisplatin ($p < 0.001$). No significant difference in antineuroblastoma activity was found among complexes **2**−**5** ($p < 0.99$). Complex **1** was significantly less active than cisplatin, with an IC50 of 245.4 ± 14.7 μM.

Cytotoxicity on Neuroblastoma and Nonmalignant Cells. In addition to the growth-inhibition activity, we studied cytopathological changes (shrinkage, round-up, and detachment) on the cells treated with gallium(III) complexes (50 μM) for 24 h. Change was observed to different extents with **2**−**5.** Growth of the neuroblastoma cells was suppressed by treatment with cisplatin (60 μM), with less-prominent cytopathological effects than those observed on cells treated with **3**−**5**. No significant cytopathological effects were observed on the studied cells treated with ionic gallium(III) at a concentration of 200 μM. This suggests that the ion itself does not play a major role in the cytotoxicity observed for complexes **2**−**5**. Representative microscopic images showed shrinkage, spherical morphology, and detachment of the cells and are seen in Figure 3. No such effects were observed for **1**.

Table 3: Apoptosis of BE(2)-C Cells Treated with **1**−**5** and Analyzed by Flow Cytometry after Staining with Annexin V-FITC and PI

Ga(III) complexes	viable cells[a]	early apoptosis[b]	late apoptosis/necrosis[c]
1	82.1 ± 10.9	12.1 ± 2.4	6.4 ± 1.8
2	54.7 ± 4.0	23.8 ± 7.4	15.6 ± 6.1
3	45.9 ± 1.9	29.7 ± 10.1	16.3 ± 4.2
4	44.0 ± 9.4	37.1 ± 22.3	17.8 ± 9.9
5	40.1 ± 6.6	45.2 ± 13.2	11.5 ± 5.0
cisplatin	27.1 ± 8.9	18.8 ± 8.8	43.8 ± 4.7
negative control	84.7 ± 5.5	6.1 ± 1.9	4.8 ± 2.0

[a] Annexin V−/PI−. [b] Annexin V+/PI−. [c] Annexin V+/PI+.

To evaluate cytotoxicity of the gallium(III) complexes on nonmalignant cells, human fibroblasts were treated with **1**−**5** for 24 h at various concentrations followed by evaluation of cytopathological effects on the microscope. Complexes **2**−**5** were found to be nontoxic at 25 μM but showed cytopathological effects upon an increase in drug concentrations to ≥50 μM. As expected, **1** was not cytotoxic on human fibroblasts at concentrations as high as 100 μM.

Apoptosis Induction on Neuroblastoma Cells. Strong apoptosis-induction activity on these cells was observed for **3**−**5** (Table 3). Complex **2** showed considerably less activity. As expected, the cells in the positive control (treated with cisplatin at a concentration of 60 μM) were necrotic or late apoptotic (Annexin V-FITC+/PI+), whereas the majority of the cells in negative control (treated with an equal amount of 5% DMSO) were viable; they stained negative for both Annexin V-FITC and PI.

Strong growth inhibition by **2**−**5** suggests that the complexes may suppress proliferation of the neuroblastoma cells via a mechanism different from that of cisplatin, in which chloro groups are exchanged by labile water ligands, allowing for coordination of the metal center to the DNA.[21] An alternative mechanism based on π-interactions of the

aromatic rings in the complexes with the DNA could explain the role played by the phenol substituents, because the role of the metal might be restricted to structural. Although this discussion is rather speculative, these compounds hold potential as effective drugs for the treatment and monitoring of neuroblastoma cancers refractory to conventional platinum-based chemotherapy. In addition to growth-inhibition activity, **3**−**5** were found to induce apoptosis of the neuroblastoma cells as demonstrated by Annexin/PI staining and flow cytometry and confirmed by Hoechst 33258 nuclear staining. Although apoptosis-induction activity was observed for **2**, the activity is less prevalent than that observed for **3**−**5**.

Conclusions

In this study, we synthesized gallium(III) complexes with asymmetric ligands. Complexes **1**−**5** were characterized by several spectroscopic methods, and some of these compounds have had their molecular structure characterized by X-ray crystallography. Complexes **2**−**5** showed strong growth inhibition and apoptosis-induction activity on BE(2)-C cells. We have begun to correlate molecular geometric parameters with growth inhibition and apoptosis induction. It is noteworthy that the complexes showing stronger antineuroblastoma activity are those containing electron-withdrawing groups, such as halogen substituents, or to a lesser extent, nitro substituents on the phenolate rings. The position of the substituents on the ring can be of some relevance. It is not clear what role is played by the geometry of these complexes, although the lower symmetry seen for **3** (local C_i) when compared to **1** (local D_{2h}) may be associated with their activity. New asymmetric ligands with distinct aromatic groups are under investigation in our labs to assess mechanistic aspects responsible for the growth inhibition and apoptosis.

Acknowledgment. C.N.V. thanks Wayne State University for financial support. F.P. thanks the Carman & Ann Adams Department of Pediatrics, Wayne State University, and The Fighting Children's Cancer Foundation for partial financial support. The authors thank Otto Muzik for helping with the statistical analysis of the data, Haiyuan Zhang for assistance in MTT and Annexin V-FITC/PI assays, and Steven Buck for flow cytometry.

(21) Jamieson, E. R.; Lippard, S. J. *Chem. Rev.* **1999**, *99*, 2467.

IC060106G